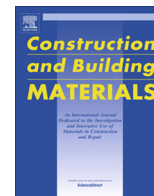




Contents lists available at ScienceDirect

Construction and Building Materials

journal homepage: www.elsevier.com/locate/conbuildmat

Tailoring Engineered Cementitious Composites with local ingredients

Hui Ma^a, Shunzhi Qian^b, Zhigang Zhang^a, Zhan Lin^a, Victor C. Li^{a,c,*}^a School of Transportation, Southeast University, Sipailou 2, Nanjing 210096, PR China^b School of Civil and Environmental Engineering, Nanyang Technological University, Singapore 639798, Singapore^c Department of Civil and Environmental Engineering, University of Michigan, 2326 G.G. Brown Building, Ann Arbor, MI 48109, USA

HIGHLIGHTS

- ECC with tensile strain capacity of 3–6% can be developed based on local ingredients.
- The Ca-content and particle size play an important role in ECC development.
- The inclusion of crumb rubber can be effective in enhancing tensile ductility in ECC.

ARTICLE INFO

Article history:

Received 27 May 2015

Received in revised form 2 October 2015

Accepted 19 October 2015

Keywords:

Material localization

Engineered Cementitious Composites (ECC)

Polyvinyl Alcohol (PVA) fiber

Micromechanics

Single fiber pullout

Strain hardening

ABSTRACT

Engineered Cementitious Composites (ECC) is a kind of High Performance Fiber Reinforced Cementitious Composites (HPFRCC) with a low fiber volume content of 2%. The unique properties of tensile strain hardening behavior and tight multiple cracks ensure that ECC can meet the stringent requirements of resiliency and durability of concrete infrastructures. While there are strong initiatives for the adoption of ECC in China, wider applications will require localization of material ingredients. In this paper, ECCs with local ingredients, including domestic PVA fibers, fly ash and crumb rubber, were developed under the guidance of micromechanics model for ECC. The fiber/matrix interface parameters and matrix parameters from single fiber pullout test and fracture toughness test respectively, were obtained for the tailoring of domestic ECC. The experimental results indicated that cost-effective ductile ECCs can be designed successfully using local material ingredients. These composites show an ultimate tensile strength of 4–5 MPa and tensile strain capacity of 3–6%.

© 2015 Elsevier Ltd. All rights reserved.

1. Introduction

Engineered Cementitious Composites (ECC), a special type of High Performance Fiber Reinforced Cementitious Composites (HPFRCC), has been researched widely since it was developed by Li and coworkers [1] in the 1990s. ECC is designed through tailoring of the fiber, matrix, and interface properties, based on the theory of micromechanics and fracture mechanics [2,3]. ECC possesses an extreme tensile ductility, in the range of 3–5% (300–500 times that of concrete or FRC) [4,5]. A typical uniaxial tensile stress–strain curve is shown in Fig. 1. After first cracking the tensile load capacity continues to rise, resulting in a macroscopic strain-hardening phenomenon accompanied by multiple micro-cracking. The crack width development is also shown in this

figure, which reveals that crack widths increase steadily up to about 60 μm , at about 1% strain. Between 1% and 5% strain, the crack width stabilizes and tends to remain constant at 60 μm while the number of cracks increases [6]. Unlike most concrete and fiber reinforced concrete materials, crack width in ECC is an intrinsic material property, independent of structural size, steel reinforcement, or the load applied to a structure built with ECC. These special properties ensure that ECC can meet the stringent requirement of resiliency and durability in infrastructures. ECC has been successfully applied in bridge deck link slab [7], bridge deck overlays, dam repair and coupling beams in high rise buildings [8,9].

Typical ECC material consists of controlled quantities and types of cement, sand, fly ash, water, additives, and short, randomly oriented polymeric fibers (e.g. Polyethylene, Polyvinyl Alcohol). Fiber volume fractions are minimized ($V_f = 1.5\text{--}2\%$) for ease of construction execution and economic feasibility in infrastructure applications [10,11]. For broader adoption of ECC in large-scale applications, the use of local materials is preferred, both for economic reasons as well as to enhance infrastructure sustainability.

* Corresponding author at: Department of Civil and Environmental Engineering, University of Michigan, 2326 G.G. Brown Building, Ann Arbor, MI 48109, USA.

E-mail addresses: huim@seu.edu.cn (H. Ma), szqian@ntu.edu.sg (S. Qian), vcli@umich.edu (V.C. Li).

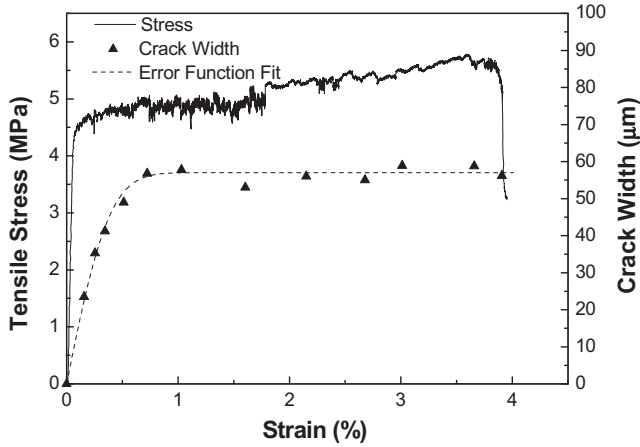


Fig. 1. Typical uniaxial tensile stress–strain–crack width curve of ECC [17] showing high tensile ductility and tight crack width.

Domestic ECCs using local raw materials and Kuraray’s PVA fiber have been developed by a number of researchers with success, including Mechtcherine and Schulze [12] in Germany and da Silva Magalhães et al. [13] in Brazil. In China, ECCs with domestic PVA fibers and other local raw materials were researched by Zhang and Qian [14], Qian and Zhang [15] and Pan et al. [16]. Zhang and Qian analyzed the feasibility of Engineered Cementitious Composites with local ingredients through four-point bending test; using domestic PVA fiber at 1.6% by volume content. Pan et al. developed ECC with a combination of domestic and imported (Kuraray Co. Ltd.) PVA fibers.

This study focuses on developing ECC with all domestic raw materials including cement, silica sand, fly ash, crumb rubber and PVA fiber. According to ECC design theory, the strain hardening behavior of ECC is largely governed by matrix fracture toughness, fiber bridging capacity and initial flaw size distribution. In this study, to tailor domestic ECC, matrix fracture toughness and fiber/matrix interfacial bond were adjusted with the addition of fly ash and crumb rubber while fiber bridging capacity was adjusted with different fiber content. The relevant parameters were obtained through single fiber pullout test and matrix fracture toughness test. In addition, the mechanical properties were assessed through compressive and uniaxial tensile test.

2. Micromechanics-based analytical models

The fundamental requirement of ECC with tensile strain hardening lies in the steady state propagation of micro-cracks emanating from material matrix defects under tensile load. The design theory of ECC was proposed by Li and coworkers [1,3,18] based on the early works of Marshall and Cox [19] on flat crack analyses of ceramics matrix composites reinforced with continuous aligned fibers. Li’s micromechanical model was further improved by Lin et al. [20], Yang et al. [21] and Kanda and Li [22]. According to this design theory, two criteria, strength criterion and energy criterion, must be satisfied for flat crack propagation to prevail over the more common Griffith crack propagation mode. First, strength criterion must be met in order to ensure an adequate fiber bridging capacity upon micro-crack initiation from a defect site. Specifically, it requires that the first cracking strength σ_{fc} controlled by matrix fracture toughness and initial flaw sizes to be less than fiber bridging capacity σ_0 on any given potential crack plane. That is

$$\sigma_{fc} \leq \sigma_0 \tag{1}$$

Furthermore, the steady-state crack propagation criterion requires the energy balance as shown in (2) [23].

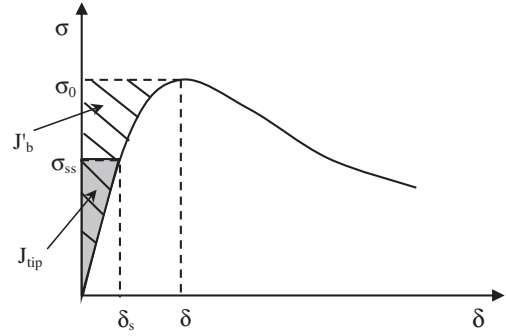


Fig. 2. Typical curve of fiber bridging stress σ – crack opening width δ .

$$\sigma_{ss}\delta_{ss} - \int_0^{\delta_{ss}} \sigma(\delta)d\delta = J_{tip} \tag{2}$$

where σ_{ss} is the steady state cracking stress; δ_{ss} is the flat crack opening corresponding to σ_{ss} (Fig. 2); J_{tip} is the crack tip toughness, which can be approximated as the cementitious matrix toughness if fiber volume fraction is less than 5%, calculated as in (3); σ_0 is the maximum bridging stress which corresponds to the crack opening δ_0 .

$$J_{tip} = \frac{K_m^2}{E_m} \tag{3}$$

where K_m is the matrix fracture toughness and E_m is the matrix Young’s modulus. Since the left hand side of (2) has the upper limit of

$$\sigma_0\delta_0 - \int_0^{\delta_0} \sigma(\delta)d\delta \equiv J'_b \tag{4}$$

it follows that a necessary condition for steady state cracking is

$$J_{tip} \leq J'_b \tag{5}$$

The strength criterion governs the range of flaw sizes that can be initiated to form part of the multiple micro-crack population during strain-hardening while the energy criterion governs the steady-state flat crack propagation. Tensile strain-hardening behavior could be achieved if both criteria are satisfied. Otherwise, the tension-softening behavior of common fiber reinforced concrete prevails. In addition, considering variability of fiber and flaw size distribution, Kanda and Li [24] recommended that $J'_b/J_{tip} > 3$ and $\sigma_0/\sigma_{fc} > 1.45$ to ensure robust strain-hardening behavior.

3. Experimental programs

3.1. Raw materials and mixture proportions

The raw materials used in this study were all produced by local manufacturers. The ordinary Portland cement (PII 42.5R cement [25]) and fly ash (Type I [26]) meet Chinese standards. Five kinds of fly ash from different coal-fired power plants were screened for use in the investigation. The chemical compositions of the cement and fly ash are listed in Table 1. The fine silica sand of 106–212 μm has a mean size of 150 μm . The crumb rubber has a size of 180 μm and a density of 1.19 g/cm^3 . The grain size distribution of aggregates and cementitious materials are presented in Fig. 3. Two domestic PVA fibers (produced by Wanwei High-tech Co. Ltd (WW) and Bao Hualin Co. Ltd (BHL) in China) were used in this research program. As control, a PVA fiber often adopted in ECC studies (REC-15 fiber with a surface oil coating of 1.2% by weight, produced by Kuraray Co. Ltd in Japan) was included in this

Table 1
Chemical composition of cement and fly ash (weight %).

Material	SiO ₂	Al ₂ O ₃	Fe ₂ O ₃	Sum	CaO	SO ₃	P ₂ O ₅	Na ₂ O	K ₂ O	TiO ₂	MgO
Cement	21.26	7.67	2.88		57.82	4.04	5.26	0	0.78	0.21	–
Fly ash 1	54.31	35.99	2.61	92.91	1.65	1.48	0.96	0.90	0.40	0.19	1.47
Fly ash 2	48.15	30.28	5.14	83.57	7.73	1.45	1.6	0.93	1.65	1.70	1.32
Fly ash 3	56.18	31.46	3.85	91.49	2.82	0.69	0.91	1.32	1.04	0.34	1.33
Fly ash 4	52.25	27.42	4.84	84.51	7.22	1.83	0.89	0.4	1.32	1.10	2.57
Fly ash 5	54.21	22.64	7.17	83.84	8.55	1.14	0.5	1.75	1.42	1.52	1.00

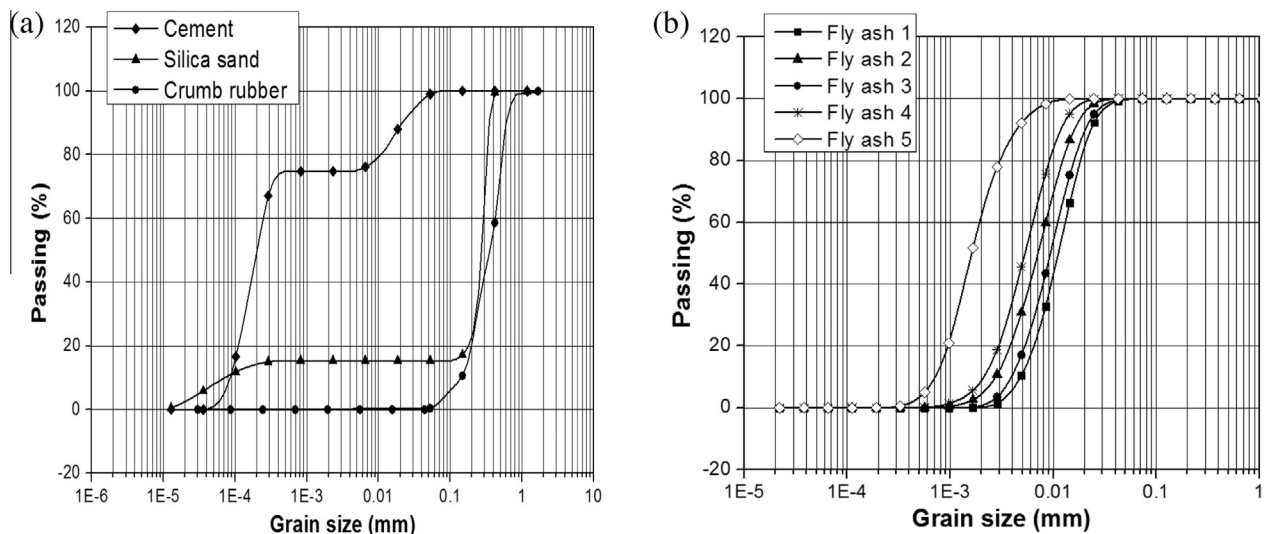


Fig. 3. Grain size distribution of domestic ECC component materials: (a) cement, silica sand and crumb rubber; (b) five different fly ashes.

study. The physical and mechanical properties of all three PVA fibers are listed in Table 2.

According to the ECC design theory summarized in Section 2, the macroscopic tensile strain hardening behavior of ECC is strongly influenced by the characteristics of fiber, matrix and fiber/matrix interface. In this study, matrix and interface properties were tailored through adjusting fly ash and crumb rubber content. In total, the test matrix includes fourteen ECC mixtures as listed in Table 3. D0 was prepared with REC-15 fiber as a reference mix. D1 has the same mix composition as D0, but with REC-15 fiber directly substituted with domestic PVA fibers. The mixtures D1 to D5 form the first test series and were prepared with different fly ash to cement ratios (FA/C) (1.2, 1.5, 2.2, 3.0 and 4.0) to adjust matrix fracture toughness and fiber/matrix interfacial bond. D6 to D8 form the second test series and were prepared by partially replacing silica sand with crumb rubber, whereby volume replacement percentage was 15%, 25% and 35%, respectively. The ECC mixtures with WW fiber and BHL fiber were designated as D#W and D#B, respectively. The fiber contents in D0 to D8 were all 2% by mixture volume. In addition, D9 to D13 repeat the test series of D4 to D8 but with a higher WW fiber content of 2.5%. This forms the third test series.

3.2. Specimen preparation and experimental tests

All ECC mixtures were prepared using a planetary mixer with 10 L capacity. All solid ingredients, including cement, silica sand, fly ash and crumb rubber, were first mixed for 3 min. Then water and high range water reducing admixture were added and mixed for 5 min. When the fresh mortar reached a uniform state, the PVA fiber was added slowly and mixed for 10 more minutes until the fibers were evenly distributed. All specimens were de-molded after 24 h, and then cured under sealed condition at $95 \pm 5\%$ RH and temperature of 20 ± 2 °C in the first seven days followed by curing in air at room temperature ($50 \pm 5\%$ RH and 20 ± 2 °C) until the predetermined testing age of 28 days (all curing time combined).

For the purpose of composite design using the multi-scale design framework of ECC, microscopic and mesoscopic parameters were experimentally determined. Fiber/matrix interfacial parameters, including chemical bond strength G_d , frictional bond strength τ_0 and slip-hardening coefficient β , were measured by single fiber pullout test. In the test, a single fiber with an embedment length of 1 mm was pulled out from a small block of matrix with dimensions of $10 \times 5 \times 1$ mm, as shown in Fig. 4. The test was conducted under

Table 2
Physical and mechanical properties of PVA fibers.

PVA fiber type	Diameter (μ m)	Length (mm)	Elongation (%)	Density (g/cm^3)	Elastic modulus (GPa)	Tenacity (MPa)
WW	35	12	7.3	1.3	31.3	1287
BHL	39	12	7	1.3	22	1250
REC-15	39	12	7	1.3	42.8	1620

Table 3
Mix design of domestic ECCs (weight ratios).

Mix ID	C	S/(C + FA)	FA	CR [*]	W/(C + FA)	HRWRA	PVA fiber (by volume)
D0	1	0.36	1.2	–	0.25	0.02	2%(REC-15)
D1(W/B)	1	0.36	1.2	–	0.25	0.02	2%(WW/BHL)
D2(W/B)	1	0.36	1.5	–	0.25	0.02	2%(WW/BHL)
D3(W/B)	1	0.36	2.2	–	0.25	0.02	2%(WW/BHL)
D4(W/B)	1	0.36	3.0	–	0.25	0.02	2%(WW/BHL)
D5(W/B)	1	0.36	4.0	–	0.25	0.02	2%(WW/BHL)
D6(W/B)	1	0.31	2.2	15%	0.25	0.02	2%(WW/BHL)
D7(W/B)	1	0.27	2.2	25%	0.25	0.02	2%(WW/BHL)
D8(W/B)	1	0.24	2.2	35%	0.25	0.02	2%(WW/BHL)
D9W	1	0.36	3.0	–	0.25	0.02	2.5%(WW)
D10W	1	0.36	4.0	–	0.25	0.02	2.5%(WW)
D11W	1	0.31	2.2	15%	0.25	0.02	2.5%(WW)
D12W	1	0.27	2.2	25%	0.25	0.02	2.5%(WW)
D13W	1	0.24	2.2	35%	0.25	0.02	2.5%(WW)

The bolded numbers signify the changes in material composition within each test series.

^{*} Crumb rubber replacement level of silica sand by volume.

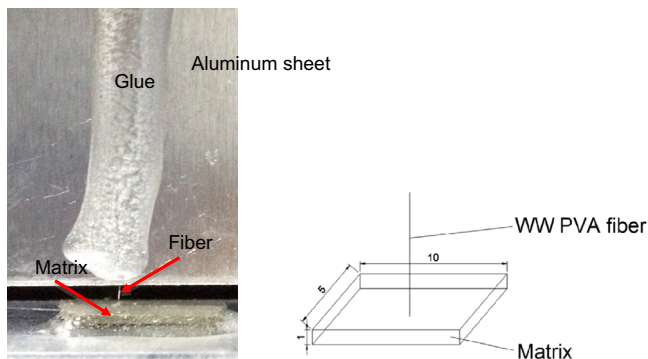


Fig. 4. Single fiber pullout test setup (all dimension in mm).

a displacement control of 0.4 mm/min. The test configuration, data interpretation and calculation procedure of the interfacial parameters follow those of Redon et al. [27]. Furthermore, the matrix (ECC without fiber) fracture toughness K_m was measured by three-point bending test following a procedure similar to that described in ASTM E399 [28]. The fracture toughness obtained based on this method is reliable for cement based material and mortar with maximum aggregate size of 1 mm [29]. The fracture toughness specimens measure $350 \times 76 \times 38$ mm, with a span of 304 mm between supports (Fig. 5). The notch depth to height ratio was 0.4. The test was executed under a displacement control rate of 0.06 mm/min.

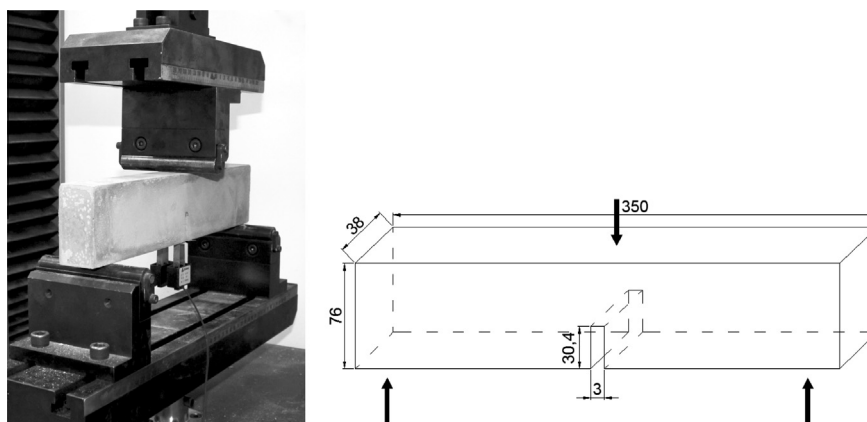


Fig. 5. The setup of three-point bending test (all dimension in mm).

The mechanical properties of ECC mixtures under compression and tension were investigated in this study. All specimens were tested at the age of 28 days. For each ECC mixture, three cube specimens with a size of $75 \times 75 \times 75$ mm were prepared for compressive test. The tensile setup and the geometry of specimen are shown in Fig. 6. Two LVDTs were fixed on both sides of the specimen to measure the deformation and the test was conducted under displacement control of 0.5 mm/min as recommended by the Japan Society of Civil Engineers (JSCE) [30].

4. Results and discussions

4.1. Fly ash type prescreening

As a matrix ingredient, fly ash is known to have a significant influence on ECC performance. It is known [31,34] that fly ash can lower the matrix fracture toughness, enhance the mix workability and improve fiber dispersion efficiency, and modifies the fiber/matrix interface. It is also well known that fly ash from different sources can have different chemical compositions and reactivity.

Five different fly ashes locally available (Table 1) were screened for producing domestic ECCs. For this screening study, REC-15 PVA fiber was used and the fly ash to cement ratio was fixed at 2.2. The tensile properties of the five mixtures are shown in Fig. 7. It can be seen that the ECC specimens with fly ash 1 and 3 show low tensile strain capacity and strength, while ECC specimens with fly ash 4 and 5 reveal a better tensile strain hardening behavior. ECC with fly ash 5, in particular, shows a relatively high tensile strain

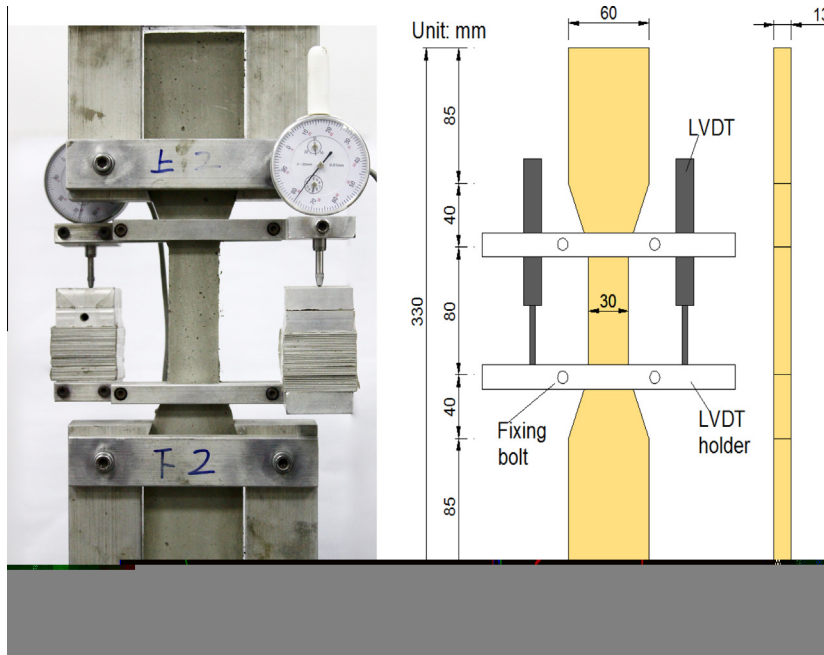


Fig. 6. The direct uniaxial tensile test: (a) test setup and (b) specimen dimension.

on PVA fiber surface and subsequently the chemical bond G_d , which enhances tensile strain capacity for ECC with fly ash 5.

Based on the above screening study, ECC with fly ash 5 exhibits better tensile strain hardening behavior than others. Hence, fly ash 5 was adopted for the tailoring of domestic ECC in the rest of this study.

4.2. Direct replacement of REC-15 fiber by domestic fibers

Once the type of fly ash was selected based on the above-described screening test, domestic PVA fibers (WW and BHL fiber) were incorporated to develop ECC material in Mixture D1 (Table 3) while Kuraray fiber (REC-15) was used as control in Mixture D0. These mixes have identical mix composition based on the work of Li and coworkers [34,35] that has resulted in highly ductile ECC known as version M45, with FA/C = 1.2. The typical uniaxial tensile stress-strain curves of ECCs with REC-15 fiber, WW fiber and BHL fiber are shown in Fig. 8.

Fig. 7. Different locally available fly ash (at FA/C = 2.2) strongly influences the tensile response of ECC (containing 2% REC-15 PVA fiber).

capacity and ultimate tensile strength over 5% and 5 MPa, respectively. As can be seen in Table 1 and Fig. 3b, fly ash 4 and 5 has relatively higher calcium content (still Type F though) and smaller particle size, which makes them more reactive [32]. Therefore, the ECC with fly ash 4 and 5 has a higher first cracking strength. Composites with fly ash 2 may not have done as well despite its high Ca content, due to its larger particle size compared with fly ash 4 and 5.

PVA fiber has a hydrophilic surface and is known to have excessive bonding to cement [33]. According to Wang and Li [34], the chemical bond of PVA fiber to matrix is governed by the metal cation concentration at the interface, in particular Al^{3+} and Ca^{2+} . In fly ash based mixture, the Al_2O_3 in fly ash can react with $Ca(OH)_2$ to form calcium aluminate hydrates (Pozzolanic reaction). Hence, the fly ash with lower combined Al_2O_3 and CaO content, e.g. fly ash 5, tends to reduce the concentration of Al^{3+} and Ca^{2+}

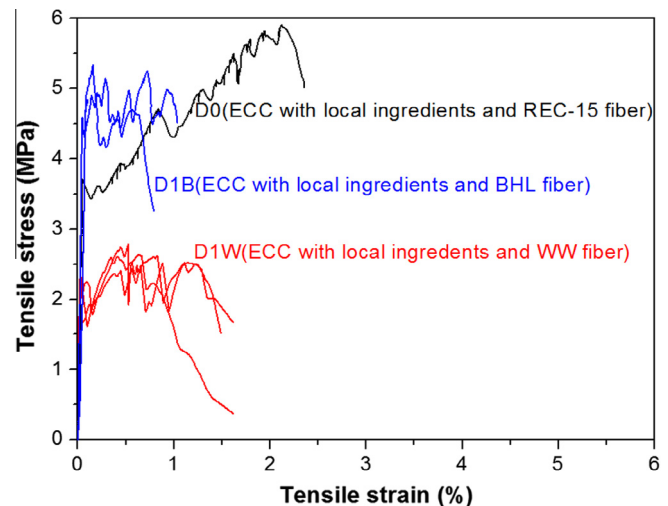


Fig. 8. Tensile behavior of ECCs with local matrix ingredients and identical composition except for PVA fiber type (REC-15, WW and BHL).

As can be seen, ECCs with WW fiber and BHL fiber exhibit unsatisfactory tensile strain-hardening behavior with a tensile strain capacity of 1.2% and 0.8%, which is significantly lower compared to that of ECC with REC-15 fiber. Furthermore, the ECC with BHL fiber have an average ultimate tensile strength of 5 MPa that is comparable to ECC with REC-15 fiber, whereas ECC with WW fiber shows a lower tensile strength of 2.6 MPa. It suggested that BHL fiber has a higher fiber bridging capacity than WW fiber in ECC.

This preliminary study indicates that ECCs using a direct substitution of REC-15 fiber with domestic PVA fiber (WW and BHL fibers) result in limited tensile ductility. Thus, composition tailoring based on micromechanics analytical models is necessary in order to produce composites with good tensile ductility using local ingredients.

4.3. Micromechanics-based design of domestic ECC

In the literature, it has been observed that high content of fly ash tends to reduce the fiber/matrix interfacial bond of PVA fiber in ECC, thus preventing excessive fiber rupture and facilitating high ductility of ECC [31,34,36]. In addition, incorporating fine size crumb rubber in ECC mixtures reduces matrix toughness and, in turn, may increase tensile strain capacity of ECC [37,38]. In this study, these two tailoring tools were used to develop domestic ECC.

Due to unavailability of continuous BHL fiber, only WW fiber was used in single fiber pullout test to derive the fiber/matrix interface micromechanical parameters. Fig. 9 shows the typical pullout curve obtained from a single fiber pullout test in D1 matrix. From this figure, the chemical bond G_d , frictional bond strength τ_0 and slip-hardening coefficient β , were calculated. Fiber bridging stress–crack opening relationship can be computed based on these parameters [21] using MATLAB, as shown in Fig. 10, which can be used to obtained fiber bridging capacity σ_0 and calculate complementary energy J_b .

Previous work [27] indicates that PVA fiber tends to reveal an extraordinary slip-hardening response during pulled out from matrix; slip-hardening coefficient β was introduced to describe this behavior [39]. However, the slip-hardening coefficient β derived in this study was found to be negligible, which suggests that WW fiber has no slip-hardening response during pull-out from the matrix with local ingredients.

The influences of fly ash on fiber/matrix interfacial parameters and matrix parameters of domestic ECC are shown in Fig. 11. The frictional bond strength τ_0 shows a general decreasing trend with

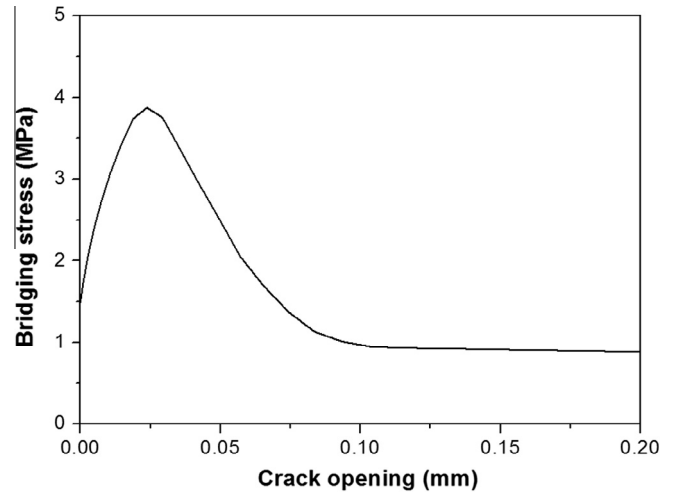


Fig. 10. Computed fiber bridging stress–crack opening relationship (σ – δ) of ECC D1 with WW fiber.

increase in fly ash content, while the chemical bond G_d remains constant at low fly ash contents, but decreases with higher fly ash contents. It indicates that fly ash in ECC mixture can reduce the fiber/matrix interface bond because of its lower chemical reactivity than that of cement. A similar trend can also be observed for matrix fracture toughness K_m and elastic modulus E_m except for FA/C = 2.2 (D3W), as shown in Fig. 11b.

Incorporation of crumb rubber has a similar influence on fiber/matrix interface and matrix parameters, as shown in Fig. 12. The chemical bond G_d is governed by the concentration of reactive cement species surrounding the fiber; while the frictional bond strength τ_0 is controlled by the microstructure of interfacial transition zone. Incorporation of crumb rubber leads to reduction of both bonds likely due to its dilution effect on reactive cement species surrounding fibers and porosity increase of the matrix [37].

Based on the micromechanics based analytical models described in Section 2, the performance indicators of strain hardening (σ_0/σ_{fc} , J_b/J_{tip}) were calculated and listed in Table 4, for the two test series D1W–D5W with increasing FA/C, and D6W–D8W with increasing crumb rubber replacement level. In this table, the σ_{fc} was obtained from the uniaxial tensile test for matrix specimen without PVA fiber; σ_0 and J_b were obtained from the fiber bridging stress–crack opening curves derived using the measured interface bond properties G_d , τ_0 and β . J_{tip} was calculated as in Eq. (3) using the measured K_m and E_m values.

From Table 4, it can be seen that the computed fiber bridging capacity σ_0 decreases slightly with the increase of fly ash content, while the first cracking strength σ_{fc} shows a significant drop to 1.8 MPa at FA/C = 4.0 (D5W), half of that at FA/C = 1.2 (D1W). This is desirable from the strength criterion viewpoint since σ_0/σ_{fc} increases from 1.08 at FA/C = 1.2 (D1W) to 1.94 at FA/C = 4.0 (D5W). Complementary energy J_b has a gradual increase while crack tip toughness J_{tip} clearly decreases with fly ash content increase. Therefore, the energy criterion Eq. (5) can be met after FA/C = 2.2 (D3W). The ratio of J_b/J_{tip} is only 0.64 at FA/C = 1.2 (D1W), which is the reason behind the observed poor strain hardening behavior of D1W.

The influence of crumb rubber on performance indicators of strain hardening is also presented in Table 4, for the test series including D3W and D6W to D8W. Similar to the influence of fly ash, fiber bridging capacity σ_0 also decreases with the increase of crumb rubber content. Complementary energy J_b increases gradually with the increase of crumb rubber content. The crack tip toughness J_{tip} drops by 20% (from 20.3 J/m² to 15.8 J/m²) when

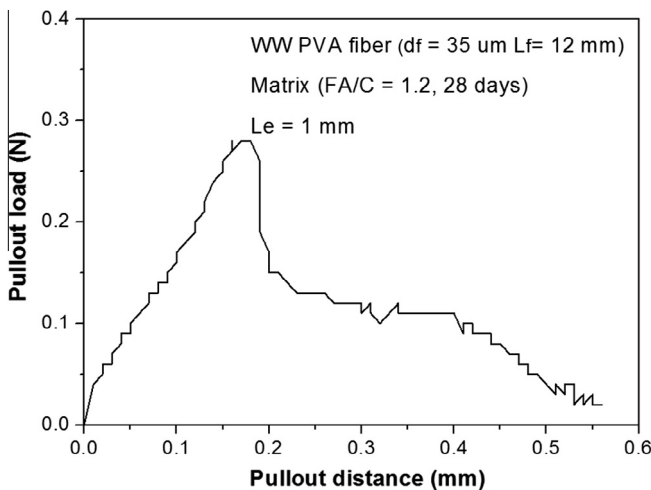


Fig. 9. Typical pullout curve of WW fiber from D1 matrix.

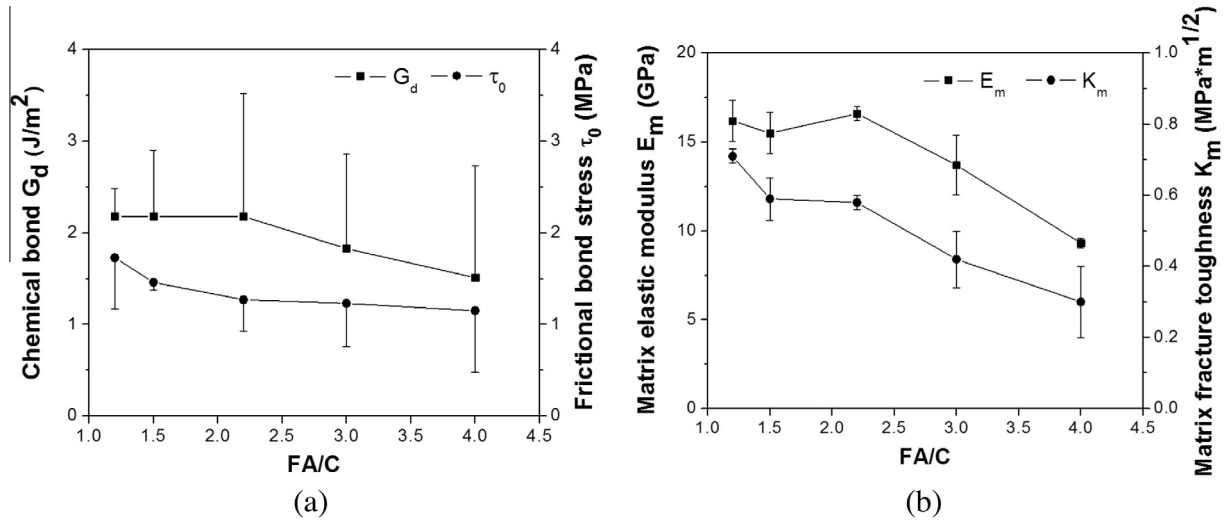


Fig. 11. Influence of fly ash on fiber/matrix interface parameters and matrix parameters: (a) G_d and τ_0 ; (b) E_m and K_m .

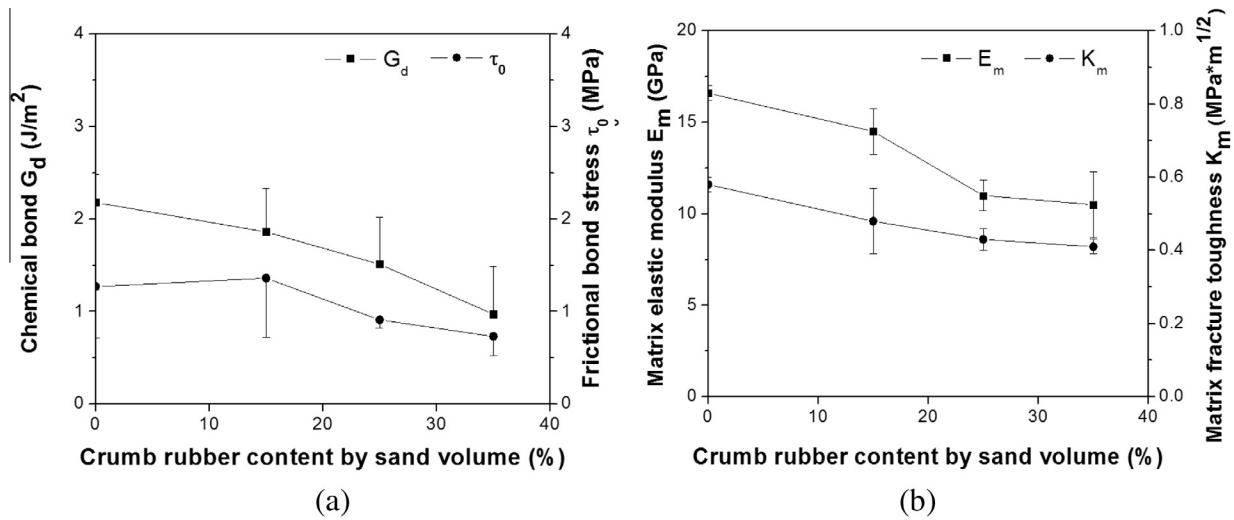


Fig. 12. Influence of crumb rubber on fiber/matrix interface parameters and matrix parameters: (a) G_d and τ_0 ; (b) E_m and K_m .

Table 4

Strain-hardening performance indicators of ECCs with WW fiber.

Mixture ID	FA/C	CR	σ_0 (MPa)	σ_{fc} (MPa)	J'_b (J/m ²)	J_{tip} (J/m ²)	J_b/J_{tip}	σ_0/σ_{fc}
D1W	1.2	–	3.9	3.6	19.8	31.1	0.64	1.08
D2W	1.5	–	3.7	2.4	21.3	22.5	0.95	1.54
D3W	2.2	–	3.6	2.5	22.9	20.3	1.13	1.44
D4W	3.0	–	3.6	2.0	23.8	12.9	1.84	1.80
D5W	4.0	–	3.5	1.8	26.0	9.7	2.68	1.94
D6W	2.2	15%	3.7	1.9	23.7	15.8	1.50	1.95
D7W	2.2	25%	3.3	2.2	27.1	16.8	1.61	1.50
D8W	2.2	35%	2.9	1.5	27.8	16.0	1.74	1.93

15% volume of silica sand was replaced by crumb rubber, after which it shows a slight fluctuation with further increase in crumb rubber replacement level (from 15% to 35%). The resulting strain hardening potential indicator J_b/J_{tip} increases gradually with the crumb rubber replacement level.

The above micromechanics parametric evaluations suggest that for ECC based on local ingredients, it is desirable to increase fly ash and crumb rubber content to achieve high tensile ductility.

4.4. Composite compressive strength

The research findings in Section 4.2, although derived from interface properties using WW fiber only, suggest a preference of tailoring the ECC matrix with high contents of fly ash and crumb rubber, for targeted high tensile ductility. However, compressive strength consideration will likely limit both fly ash and crumb rubber contents. In this section, the compressive strength of the two

test series, (D1W/B–D5W/B) with increasing FA/C, and (D3W/B, D6W/B–D8W/B) with increasing CR at fixed FA/C, are reported.

The compressive strengths of ECCs with WW/BHL fiber and different fly ash content are shown in Fig. 13. The compressive strength shows a slight reduction when the FA/C increases from 1.2 to 2.2, and a significant drop when the FA/C increases from 2.2 to 4.0.

Similarly, the compressive strength decreases gradually with the increase of crumb rubber (Fig. 14), which can be attributed to the fact that crumb rubber has lower strength and poor bond with the hydration products compared to that of silica sand. Another possible reason is the increase in matrix porosity caused by the incorporation of crumb rubber.

From this study of domestic ECC, FA/C content should not exceed 3.0 if a compressive strength of around 30 MPa is desired. When crumb rubber is added, a further lowering of compressive strength to around 20–25 MPa results, approaching the lower limit of a structural concrete.

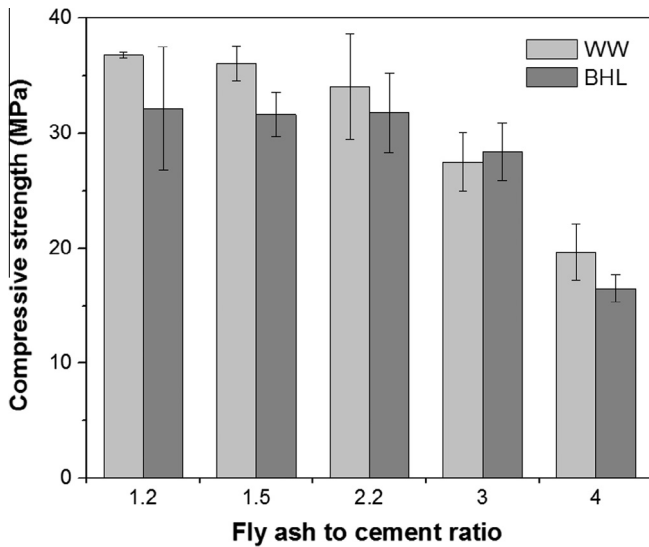


Fig. 13. Compressive strength of ECCs with different fly ash content (Series D1W/B–D5W/B).

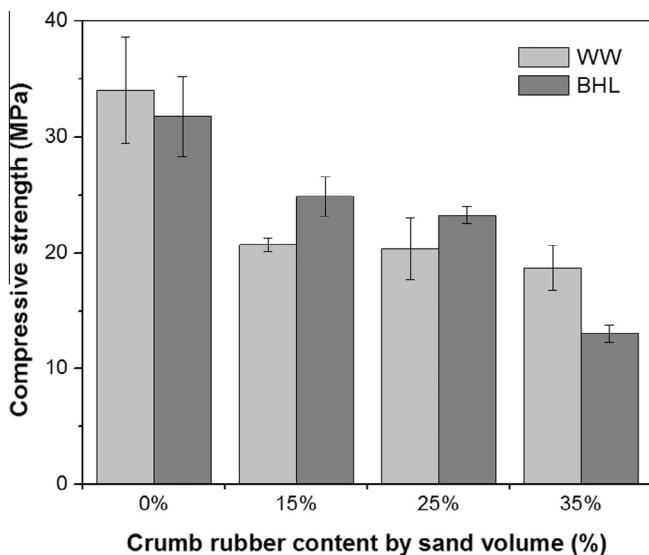


Fig. 14. Compressive strength of ECCs with different crumb rubber content (Series D4W/B, D6W/B–D8W/B).

4.5. Composite tensile properties

From the above studies on micromechanics of tensile behavior and compressive strength measurement of domestic ECCs, it appears that an optimal mix composition would have FA/C = 3.0 with no crumb rubber content, for both BHL and WW fiber. This mix is expected to produce ductile tensile properties while maintaining reasonable compressive strength. To verify this expectation, direct tensile tests of the two test series (with and without crumb rubber) and with each fiber type were carried out.

The tensile behavior of the two test series are shown in Figs. 15 and 16. As can be seen in Fig. 15, significant strain hardening is observed for ECC mixtures with different fly ash content. The tensile strain capacity of ECC with WW fiber and BHL fiber is almost the same at the respective fly ash content, and increases significantly with the fly ash content, from 1.5% at FA/C = 1.2 (D1) to 4.5% at FA/C = 4.0 (D5). The result is consistent with the increase in the ratio J_b/J_{tip} (Table 4) which is regarded as the strain hardening potential indicator for ECC material [40].

Consistent with the decrease of fiber bridging capacity σ_0 with increasing fly ash content presented in Table 4, a general reduction trend is observed for ultimate tensile strength in Fig. 15, except for D2B. Nevertheless, the ultimate tensile strength of domestic ECC at FA/C = 4.0 (D5B) can still reach 4.5 MPa for BHL fiber. On the other hand, ECCs with WW fiber exhibit relatively low ultimate tensile strength. As mentioned in Section 4.1, it suggests that BHL fiber in ECC provide a higher fiber bridging capacity when compared with WW fiber. According to Li et al. [33], the peak value of $\sigma(\delta)$ curve is governed by fiber content V_f , fiber diameter d_f , fiber length L_f and fiber/matrix interface frictional stress τ_0 . The WW fiber and BHL fiber have similar d_f , the same L_f and V_f , and very similar fiber strength (Table 2). Further, microscopic examination of the fracture surface indicates that fibers are pulled out rather than rupture. Hence, τ_0 appears to be the dominating factor that causes the difference of ultimate tensile strength of composites with WW and BHL fiber.

The τ_0 value for BHL was not measured due to unavailability of continuous BHL fibers for direct single fiber pull-out test. However, an estimation of τ_0 can be obtained from the measured peak bridging strength σ_0 . Wang and Li [34] showed that τ_0 and σ_0 are linearly related, as in Eq. (6), which ignores fiber rupture, slip-hardening, and snubbing effect for simplicity.

$$\sigma_0 = \frac{4V_f\tau_0}{L_f d_f} \left(\frac{L_f}{2}\right)^2 \cdot \eta_B \quad (6)$$

The orientation effect captured by η_B defines the efficiency of fiber bridging [21]. When fibers are uniformly random in 3D and 2D, η_B is 1/2 and $2/\pi$, respectively [41]. Hence τ_0 of BHL fiber can be deduced from Eq. (6) based on measured σ_0 . As can be seen from Table 5, the τ_0 of BHL fiber is larger than that of WW fiber in most cases.

Fig. 16 shows the influence of crumb rubber on the tensile behavior of ECC with WW and BHL fiber, respectively. As seen in Fig. 16a, the tensile strain hardening behavior of ECC with WW fiber is improved significantly. Its tensile strain capacity increases from 1.5% to above 6% after incorporating crumb rubber, increasing by 270%. Especially, the tensile strain capacity reached 7% when crumb rubber content is 35% by volume replacement of silica sand.

For ECC with BHL fiber, the ultimate tensile strength reduces significantly from 5.5 MPa to 3.5 MPa after incorporation of crumb rubber while the tensile strain capacity remains more or less the same, as shown in Fig. 16b. Based on the results from Table 4, J_{tip} reduces with the introduction of crumb rubber into ECC matrix. The unchanged tensile ductility suggests a similar descending trend for J_b so that J_b/J_{tip} remains essentially constant.

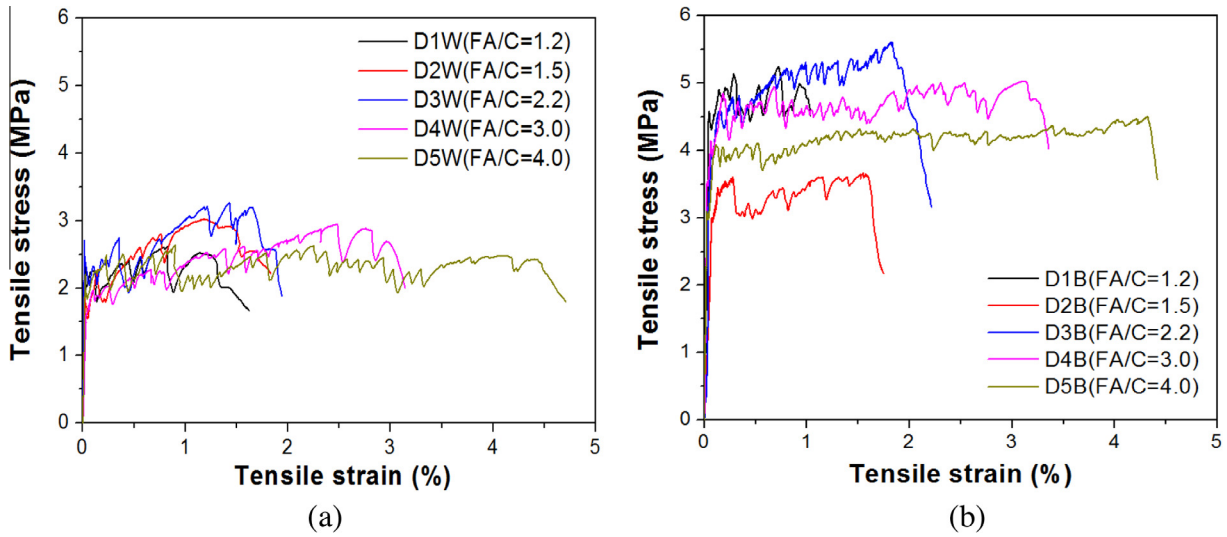


Fig. 15. Uniaxial tensile stress–strain curves of ECCs with different fly ash content and with no crumb rubber: (a) WW fiber (Series D1W–D5W); (b) BHL fiber (Series D1B–D5B).

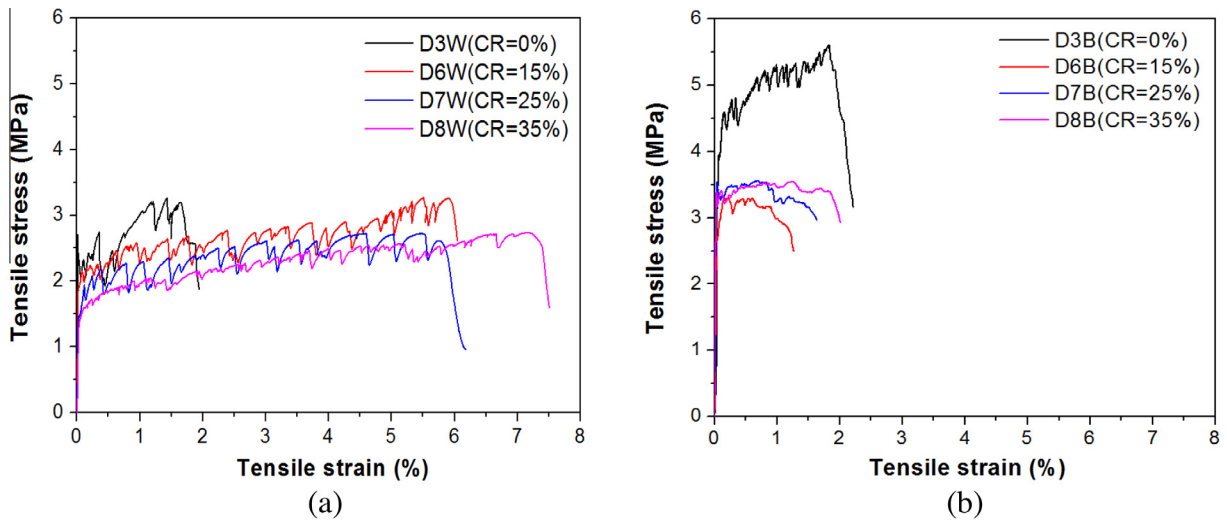


Fig. 16. Uniaxial tensile stress–strain curves of ECCs with different crumb rubber content and with fixed FA/C = 2.2: (a) WW fiber (Series D3W, D6W–D8W); (b) BHL fiber (Series D3B, D6B–D8B).

Table 5

The τ_0 (MPa) of BHL fiber (deduced) and WW fiber (measured).

Mixture ID	BHL (2D)	BHL (3D)	WW
D1	1.36	1.73	1.73
D2	0.95	1.22	1.46
D3	1.49	1.91	1.27
D4	1.36	1.73	1.23
D5	1.22	1.57	1.15
D6	0.95	1.22	1.36
D7	0.95	1.22	0.91
D8	0.95	1.22	0.73

The above results indicate that the tensile strain capacity of domestic ECCs increase with increasing fly ash content as anticipated by micromechanics (Section 4.2). Incorporation of crumb rubber enhances the tensile strain capacity of ECC with WW fiber but not for BHL fiber.

While the uniaxial tensile stress–strain behavior experimentally measured confirmed that tensile ductility is achieved, the data suggest that for the composite containing BHL fiber, a

FA/C = 3.0 provides a good balance between tensile and compressive properties. For the composite containing WW fiber, the combination of FA/C = 2.2 and CR = 15% seems to generate a high ductile ECC, but with some sacrifice in compressive strength, dropping to below 30 MPa at 28 days.

Due to the slow reactivity of fly ash, it is anticipated that the compressive strength and ultimate tensile strength would increase with age beyond 28 days, while tensile strain capacity would decrease. From this viewpoint, the compositions D5W, D5B and D6W may be desirable for domestic ECC if early age strength is not so critical in a particular application. Further studies on these composites at 90 days, 180 days and 540 days will be reported separately.

The low tensile strength of domestic ECCs with WW fiber may restrict their application; in the next section the strategy of high fiber volume content was attempted to overcome this deficiency.

4.6. Domestic ECC with different fiber content

Theoretically, the fiber bridging capacity (and the composite tensile strength) is governed by fiber strength, fiber content, and

interfacial properties (G_d and τ_0). Therefore, a slightly higher fiber content (2.5% by volume) was attempted with domestic ECCs D9W and D10W, in addition to high fly ash content (FA/C = 3.0 and 4.0). The same approach was also adopted in domestic ECCs D11W and D13W with the incorporation of crumb rubber.

The performance indicators of strain hardening of ECCs containing WW fibers are listed in Table 6. Also the σ_{fc} was obtained from the uniaxial tensile test for matrix specimen without PVA fiber; σ_0 and J'_b were obtained from the fiber bridging stress – crack opening curves; J_{tip} was calculated as in (3). It can be seen that fiber bridging capacity σ_0 and complementary energy J'_b increase when the fiber content increases to 2.5% by volume, resulting in improved

J'_b/J_{tip} and σ_0/σ_{fc} . Theoretically larger strain hardening index should be conducive to tensile strain hardening behavior, assuming all fibers are randomly distributed.

Figs. 17 and 18 illustrate the influence of higher fiber content on tensile strain hardening behavior of domestic ECCs. As can be seen in Fig. 17a, domestic ECC (without crumb rubber) D9W exhibits an excellent strain hardening behavior with tensile strain capacity of 6% and ultimate tensile strength of 4 MPa, an increase of 100% and 33% compared with domestic D4W, respectively, for FA/C = 3.0. Fig. 17b shows that the tensile strain capacity increases by 67% (from 4.5% to 7.5%), and the ultimate tensile strength increases from 2.5 MPa to 3.2 MPa when the fiber content increases to 2.5%

Table 6
Performance indicators of strain hardening for ECCs when (WW) fiber content is increased from 2.0% to 2.5%.

Mixture ID	σ_0 (MPa)	σ_{fc} (MPa)	J'_b (J/m ²)	J_{tip} (J/m ²)	J'_b/J_{tip}	σ_0/σ_{fc}
D4W/D9W	3.6/4.5	2.0	23.8/29.8	12.9	1.84/2.25	1.80/2.31
D5W/D10W	3.5/4.4	1.8	26.0/31.9	9.7	2.68/3.29	1.94/2.44
D6W/D11W	3.7/4.6	1.9	23.7/29.7	15.8	1.50/1.88	1.95/2.42
D7W/D12W	3.3/4.0	2.2	27.1/33.4	16.8	1.61/1.99	1.50/1.82
D8W/D13W	2.9/3.6	1.5	27.8/34.7	16.0	1.74/2.17	1.93/2.40

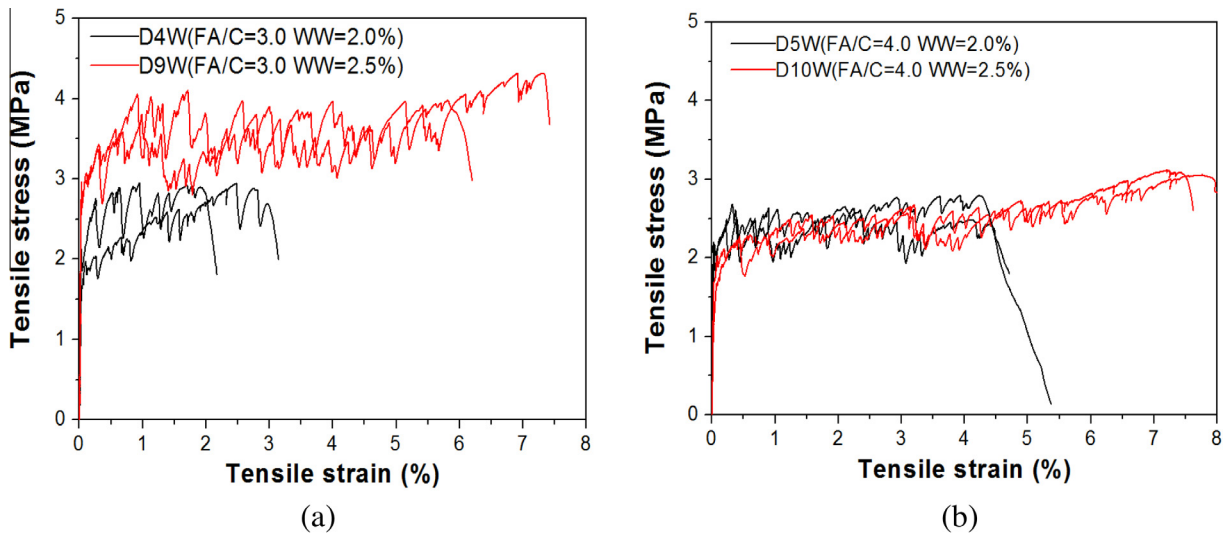


Fig. 17. Uniaxial tensile stress–strain curves of ECCs with different WW fiber content: (a) FA/C = 3.0 (D9W vs D4W); (b) FA/C = 4.0 (D10W vs D5W).

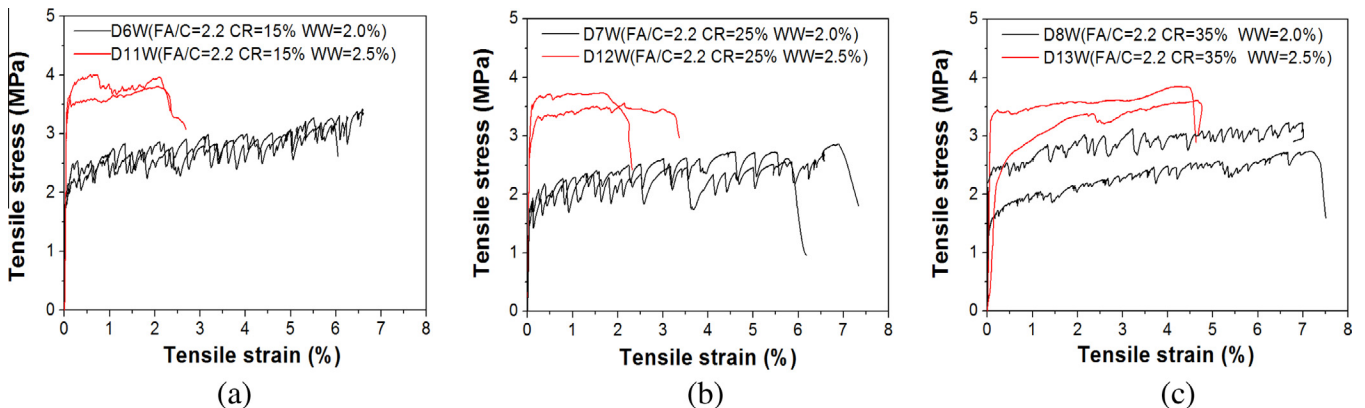


Fig. 18. Uniaxial tensile stress–strain curves of ECCs with different fiber content: (a) CR = 15% (D11W vs D6W); (b) CR = 25% (D12W vs D7W) and (c) CR = 35% (D13W vs D8W).

from 2.0% by volume (D10W vs D5W), for FA/C = 4.0. The compressive strength for D9W and D10W reached 29 and 23 MPa, respectively.

For mixes D11W to D13W (containing crumb rubber) with higher fiber content, both first cracking strength and ultimate tensile strength have a significant increase compared with D6W to D8W (Fig. 18). However, the tensile strain capacities of D11W to D13W show a pronounced reduction. It may be attributed to the difficulty of mixing when incorporating high volume of fiber and crumb rubber while maintaining fixed water to binder ratio, which negatively impacts the fiber dispersion in ECC mixtures. The poor fiber dispersion causes the reduction of tensile strain capacity, which explains the inconsistency between the predicted higher ductility (indicated by increase of strain hardening indicator ratio J_b/J_{tip}) and actual performance for these composites containing crumb rubber. However, for the higher fiber content mixes, Fig. 18 also suggests the beneficial effect of crumb rubber content which leads to higher tensile ductility, likely a result of increase in flaw population that triggers a larger number of microcracks. For D11W to D13W, the difficulty of fiber dispersion with the higher fiber content also leads to a lowering of compressive strength, to 15–18 MPa.

5. Conclusions

This study focuses on the development of ECC using Chinese domestic materials, including matrix ingredients and PVA fibers. The micromechanical model was used to guide the design of domestic ECC. The fiber/matrix interface and matrix properties with strong bearing on the tensile strain hardening behavior were tailored through the selection of fly ash type, and adjustment of fly ash and crumb rubber contents. The specific conclusions can be drawn as following:

- (1) To attain domestic ECC, fly ash with higher calcium/smaller particle size and lower combined Al_2O_3 and CaO content (e.g. fly ash 5 in this study) is found to be beneficial for higher first cracking strength and tensile ductility, respectively. The tensile ductility of ECC increases with fly ash content. However, excessive amount of fly ash tends to reduce the compressive strength of the composite. The optimal FA/C appears to be 3.0, when crumb rubber is not incorporated.
- (2) Using BHL fiber at 2%, it was found that domestic ECC with excellent tensile strain hardening behavior can be developed using only local ingredients. For this composite (D4B) tensile strain exceeding 3%, ultimate tensile strength of 5 MPa and compressive strength of 30 MPa can be achieved.
- (3) Using WW fiber at 2%, it was found that the combined use of fly ash and crumb rubber can be beneficial to composite tensile ductility. For this composite (D6W), the tensile strength and ductility reaches 3.2 MPa and 6%, respectively. However, the compressive strength of the composite is only 20 MPa due to the use of crumb rubber.
- (4) Domestic ECC (D9W) with ultimate tensile strength and tensile strain capacity exceeding 4 MPa and 6% can be achieved, when 2.5% WW fiber was used. The compressive strength for this mix is 29 MPa.

Acknowledgements

The authors would like to thank the National Natural Science Foundation of China (No. 51008071) and Nanyang Technological University for providing start-up grant (M4081208). The corresponding author also would like to thank Southeast University for the Thousand Talent Specialist Award.

References

- [1] V.C. Li, From micromechanics to structural engineering – the design of cementitious composites for civil engineering application, *J. Struct. Eng. Earthquake Eng.* 10 (2) (1993) 37–48.
- [2] V.C. Li, H. Stang, H. Krenchel, Micromechanics of crack bridging in fiber reinforced concrete, *Mater. Struct.* 26 (162) (1993) 486–494.
- [3] V.C. Li, C.K.Y. Leung, Steady state and multiple cracking of short random fiber composites, *J. Eng. Mech., ASCE* 118 (11) (1992) 2246–2264.
- [4] V.C. Li, ECC – tailored composites through micromechanical modeling, in: *Fiber Reinforced Concrete: Present and the Future* edited by Banthia et al., CSCE, Montreal 1998, 64–97.
- [5] V.C. Li, On engineered cementitious composites (ECC) – a review of the material and its applications, *J. Adv. Concr. Technol.* 1 (3) (2003) 215–230.
- [6] M.B. Weimann, V.C. Li, Drying shrinkage and crack width of ECC. *Brittle Matrix Composites-7*, Warsaw, Poland 2003, 37–46.
- [7] S. Qian, M.D. Lepech, Y.K. Yun, V.C. Li, Introduction of transition zone design for bridge deck link slabs using ductile concrete, *ACI Struct. J.* 106 (1) (2009) 96–105.
- [8] V.C. Li, Strategies for high performance fiber reinforced cementitious composites development, in: S. Ahmad, M. di Prisco, C. Meyer, G.A. Plizzari, S. Shah (Eds.), *Fiber Reinforced Concrete: From Theory to Practice*, Proceedings of the North American/European Workshop on Advances in Fiber Reinforced Concrete, Bergamo, Italy 2004, 93–98.
- [9] M. Kunieda, K. Rokugo, Recent progress on HPRFCC in Japan required performance and applications, *J. Adv. Concr. Technol.* 4 (1) (2006) 19–33.
- [10] S. Wang, V.C. Li, Polyvinyl alcohol fiber reinforced engineered cementitious composites: material design and performances, in: *Proceedings of Int'l Workshop on HPRFCC in Structural Applications*, Honolulu, Hawaii, USA, May 2005, 23–26.
- [11] V.C. Li, High performance fiber reinforced cementitious composites as durable material for concrete structure repair, *Int. J. Restor. Build. Monuments* 10 (2) (2004) 163–180.
- [12] V. Mechtcherine, J. Schulze, Testing the behavior of strain hardening cementitious composites in tension, in: *Proceedings of the International RILEM Workshop on High Performance Fiber Reinforced Cementitious Composites in Structural Applications* 2006, 37–46.
- [13] M. da Silva Magalhães, R. Dias Toledo Filho, E. de Moraes Rego Fairbairn, Influence of local raw materials on the mechanical behaviour and fracture process of PVA-SHCC, *Mater. Res.* 17 (1) (2014) 146–156.
- [14] Z. Zhang, S. Qian, The feasibility of engineered cementitious composites with local compositions, in: *Proceedings of the 2nd International RILEM Conference on Strain Hardening Cementitious Composites*, Rio de Janeiro, Brazil 2011, 323–328.
- [15] S. Qian, Z. Zhang, Development of engineered cementitious composites with local ingredients, *J. Southeast Univ. (English Edition)* 28 (3) (2012) 327–330.
- [16] Z. Pan, C. Wu, J. Liu, W. Wang, J. Liu, Study on mechanical properties of cost-effective polyvinyl alcohol engineered cementitious composites (PVA-ECC), *Constr. Build. Mater.* 78 (2015) 397–404.
- [17] V.C. Li, S. Wang, C. Wu, Tensile strain-hardening behavior of polyvinyl alcohol engineered cementitious composite (PVA-ECC), *ACI Mater. J.* 98 (2001) 483–492.
- [18] V.C. Li, H.C. Wu, Conditions for pseudo strain-hardening in fiber reinforced brittle matrix composites, *Appl. Mech. Rev.* 45 (8) (1992) 390–398.
- [19] D.B. Marshall, B.N. Cox, A J-integral method for calculating steady-state matrix cracking stresses in composites, *Mech. Mater.* 8 (1988) 127–133.
- [20] Z. Lin, T. Kanda, V.C. Li, On interface property characterization and performance of fiber reinforced cementitious composites, *Concrete Science and Engineering*, 1, RILEM, 1999, pp. 173–184.
- [21] E.H. Yang, S. Wang, Y. Yang, V.C. Li, Fiber-bridging constitutive law of engineered cementitious composites, *J. Adv. Concr. Technol.* 6 (1) (2008) 181–193.
- [22] T. Kanda, V.C. Li, Practical design criteria for saturated pseudo strain hardening behavior in ECC, *J. Adv. Concr. Technol.* 4 (1) (2005) 59–72.
- [23] E.H. Yang, V.C. Li, Numerical study on steady-state cracking of composites, *Compos. Sci. Technol.* 67 (2) (2007) 151–156.
- [24] T. Kanda, V.C. Li, Multiple cracking sequence and saturation in fiber reinforced cementitious composite, *Concr. Res. Technol., JCI* 9 (2) (1998) 19–33.
- [25] GB175-2007, Common Portland Cement, 2007 (in Chinese).
- [26] GB1596-88, Fly Ash Used in Cement and Concrete, 1988 (in Chinese).
- [27] C. Redon, V.C. Li, C. Wu, H. Hoshino, T. Saito, A. Ogawa, Measuring and modifying interface properties of PVA fibers in ECC matrix, *J. Mater. Civ. Eng. ASCE* 13 (6) (2001) 399–406.
- [28] ASTM E399-12, Standard test method for linear-elastic plane-strain fracture toughness K_{Ic} of metallic materials.
- [29] V.C. Li, D.K. Mishra, H. Wu, Matrix design for pseudo-strain-hardening fiber reinforced cementitious composites, *Mater. Struct.* 28 (1995) 586–595.
- [30] JSCE, Recommendations for Design and Construction of High Performance Fiber Reinforced Cement Composites with Multiple Fine Cracks, Japan Soc. of Civil Engineers, Tokyo, 2008.
- [31] E.H. Yang, Y. Yang, V.C. Li, Use of high volumes of fly ash to improve ECC mechanical properties and material greenness, *ACI Mater. J.* 104 (6) (2007) 303–311.
- [32] P.K. Mehta, Influence of fly ash characteristics on the strength of Portland-fly ash mixtures, *Cem. Concr. Res.* 15 (1985) 669–674.

- [33] V.C. Li, C. Wu, S. Wang, A. Ogawa, T. Saito, Interface tailoring for strain-hardening polyvinyl alcohol-engineered cementitious composite (PVA-ECC), *ACI Mater. J.* 99 (5) (2002) 463–472.
- [34] S. Wang, V.C. Li, Engineered cementitious composites with high-volume fly ash, *ACI Mater. J.* 104 (3) (2007) 233–241.
- [35] M.D. Lepech, V.C. Li, Water permeability of engineered cementitious composites, *Cement Concr. Compos.* 31 (2009) 744–753.
- [36] A. Peled, M.F. Cyr, S.P. Shah, High content of fly ash (class F) in extruded cementitious composites, *ACI Mater. J.* 97 (5) (2000) 509–517.
- [37] X. Huang, R. Ranade, W. Ni, V.C. Li, On the use of recycled tire rubber to develop low E-modulus ECC for durable concrete repairs, *Constr. Build. Mater.* 46 (2013) 134–141.
- [38] Z. Zhang, H. Ma, S. Qian, Investigation on properties of ECC incorporating crumb rubber of different sizes, *J. Adv. Concr. Technol.* 13 (2015) 241–251.
- [39] Y. Wang, V.C. Li, S. Backer, Modeling of fiber pull-out from a cement matrix, *Int. J. Cem. Compos. Lightweight Concr.* 10 (3) (1988) 143–149.
- [40] T. Kanda, V.C. Li, A new micromechanics design theory for pseudo strain hardening cementitious composite, *J. Eng. Mech., ASCE* 125 (4) (1999) 373–381.
- [41] Y. Wang, S. Backer, V.C. Li, A statistical tensile model of fiber reinforced cementitious composites, *J. Compos.* 20 (3) (1990) 265–274.